A framework for co-existence of radar and communication with joint design

Hao Mao[1], Haiyun Zhu[2], Yinghui He[1*] , Guanding Yu[1] and Rui Yin[3]

*Correspondence:
2014hyh@zju.edu.cn

[1] College of Information
Science and Electronic
Engineering, Zhejiang University,
Hangzhou 310027, China
[2] China Telecom, Beijing, China
[3] College of Information
and Electrical Engineering,
Hangzhou City University,
Hangzhou 310015, China

Abstract

The integration of both sensing and communication functions is a crucial feature for future communication systems. This paper considers a novel scenario where a radar covers multiple small-cell base stations which operate in different spectra. Due to the limited spectra resource, the radar needs to reuse the spectra of one BS for tracking. To suppress interference and improve performance, we propose a framework including two stages and the corresponding communication and sensing algorithms. Specifically, at the detection stage, we aim to minimize the system transmit power while maintaining the performance of both radar and communication. At the tracking stage, our goal is to maximize the radar sensing performance under a given power budget, while ensuring communication quality. Due to the complexity of the original problem, we address it by introducing auxiliary variables and proposing a penalty dual decomposition-based algorithm, enabling us to solve a more tractable form of the problem. In the inner loop, we propose a concave–convex procedure-based algorithm to handle the optimization problem, while adopting the block coordinate descent algorithm to iteratively update the variables. In the outer loop, we update the penalty term or Lagrange multipliers. Furthermore, we propose a radar target parameter estimation algorithm based on successive interference cancellation, which aims to mitigate communication interference. Finally, numerical simulations demonstrate the effectiveness of the proposed system, and the superior performance of our proposed algorithms over benchmark algorithms.

Keywords: Spectrum sharing, Joint design, Radar-communication coexistence, Parameter estimation

1 Introduction

With the advent of the 6 G era, the proliferation of wireless communication devices is surging, while spectrum resources remain scarce. To alleviate this contradiction, future communication systems need to explore the possibility of coexisting with other systems in the same frequency band. Meanwhile, radar technology, after decades of development, has found extensive application in fields such as aviation navigation. In order to prevent mutual interference between radar and communication systems, both systems are exploring higher-frequency bands and the potential for coexistence [1]. The matter of spectrum sharing between radar and communication systems has garnered significant interest from industry and academia in recent years [2, 3].

Currently, there are two primary research directions aimed at resolving the challenge of cooperative spectrum sharing between radar and communication: radar-communication coexistence (RCC) and dual-functional radar-communication system (DFRC). The former direction aims to develop various interference management techniques to enable simultaneous operation of the two systems [4–7]. The latter direction aims to achieve remote sensing and wireless communication using a single signal generated by a single platform [8–13]. Although the DFRC system may outperform the RCC system, developing a single waveform for two purposes poses significant complexity challenges. Therefore, this paper focuses on the RCC direction, aiming to suppress mutual interference through joint system design.

In scenarios where radar and communication systems coexist, mitigating or minimizing mutual interference presents a substantial challenge. Furthermore, harnessing the potential collaboration between radar and communication systems is crucial. Current studies have focused on exploring joint beamforming designs to enable the coexistence of radar and communication systems [14, 15]. According to the knowledge of the radar sampling scheme, a method has been proposed in [16] to design the communication transmit covariance matrix, which reduces the effective interference power at radar. In [17], the authors have employed a multi-objective optimization technique to optimize radar transmit power and allocate bandwidth in order to enhance overall system performance. In [15], the spectrum sharing between multi-user multiple-input multiple-output (MU-MIMO) communication and MIMO radar is considered, and the transmit beamformer is optimized to maximize the detection probability of the radar while maintaining communication quality. One approach for mitigating radar interference involves projecting the radar waveform into a null space [18–20]. Another approach is optimizing the radar receiving filter to mitigate interference caused by communication systems [21]. Co-design in the time domain and spatial domain has also been investigated [22–25]. Specifically, joint design of the communication transmit covariance matrix and radar sampling scheme is explored in [22, 23], formulated as a non-convex optimization problem and solved by the alternating optimization algorithm. In [24], the co-design of radar pulse and the communication matrix has been studied. *In [26], the authors consider an integrated sensing and communication system operating on a single device, and schemes are proposed to flexibly allocate the limited power and bandwidth resources.* Previous research, as seen in [22–26], has only examined two scenarios: where the radar system operates in the same spectrum with all BSs or it operates in different spectra by spectrum allocation. In this paper, we consider the dynamic spectrum sharing between the radar and communication systems. Specifically, the radar dynamically re-uses the spectrum of BSs.

In [27–29], novel frame structures for DFRC base stations (BSs) have been proposed for communication and target detection as well as tracking. In particular, the authors in [27] have developed a time division duplex (TDD) frame structure which splits the system operations into three stages: radar target search, radar transmit beamforming, and radar target tracking. Extended Kalman filtering frameworks have also been developed to track and predict parameters of vehicles while maintaining communication quality [28]. Furthermore, inspired by the frame structures in DFRC systems, we seek to investigate an effective integrated system of RCC for detection and tracking.

For target parameter estimation, [30] has proposed a waveform design method in cooperative radar-communication systems. In [31], an orthogonal time frequency space (OTFS) modulation has been investigated for joint communication and radar parameter estimation system. In [32], a practical algorithm has been investigated for interference cancellation in ZigBee communication. To the best of the author's knowledge, no existing studies have concentrated on the parameter estimation of radar target using successive interference cancellation (SIC). Furthermore, we seek to investigate an effective SIC-based method to mitigate the communication interference for parameters estimation.

To summarize, our main contributions in this paper are:

- We introduce a new spectrum sharing scenario where the radar system strategically reuses the spectrum of a specific small-cell base station (BS).
- Our proposed novel RCC frame structure realizes efficient radar target detection and tracking while simultaneously meet requirements for downlink.
- To handle the non-convex optimization problems in both stages, we reconfigure the original problems into a more manageable form by introducing auxiliary variables and proposed a penalty dual decomposition (PDD)-based algorithm, with a guarantee of convergence to a stationary point.
- To mitigate the communication interference to the radar, we propose a SIC-based algorithm for target parameter estimation. The simulation results demonstrate the superior performance of the proposed algorithm compared to the benchmark algorithms.

1.1 Organization

The structure of this paper is as follows. Section 3 introduces the framework and process of the whole system. The proposed target parameter estimation algorithm is presented in Sect. 4. Sections 5 and 6 propose the joint design schemes for the target detection and the target tracking, respectively. Numerical experiments are provided in Sect. 7, and conclusions are drawn in Sect. 8.

Notations: In this paper, lowercase letters denote scalars, e.g., a, boldface lowercase letters denote vectors, e.g., $\boldsymbol{a}$, and boldface upper letters denote matrices, e.g., $\mathbf{A}$. $\mathbf{I}$ represents the identity matrix. The conjugate operator, transpose, and Hermitian are denoted by $(\cdot)^*$, $(\cdot)^T$, and $(\cdot)^H$, respectively. For a matrix $\mathbf{A}$, $\mathrm{diag}(\cdot)$ denotes a vector whose elements are the correlated with the diagonal of $\mathbf{A}$, $\boldsymbol{a}$ denotes the Euclidean norm of $\boldsymbol{a}$, and A denotes the Frobenius norm of A. $\mathbf{0}_{m \times n}$ denotes the $m \times n$ all-zero matrix. The real value of a complex scalar is denoted by $\Re(\cdot)$ and $|\cdot|$ denotes the absolute value of a complex scalar. Moreover, we use $\mathbb{C}^{m \times n}\left(\mathbb{R}^{m \times n}\right)$ to denote the space of $m \times n$ complex-valued (real-valued) matrix. For the $m \times n$ matrix $A = [\boldsymbol{a}_1, \boldsymbol{a}_2, \ldots, \boldsymbol{a}_n]$, we define that $\mathrm{vec}(A) = [\boldsymbol{a}_1^T, \boldsymbol{a}_2^T, \ldots, \boldsymbol{a}_n^T]$.

2 Methods/experimental

In our study, the radar system coexists with multiple small-cell base stations, each operating on distinct frequency bands. Crucially, the radar only reuses the frequency band of one selected base station. This configuration ensures that interference to the radar is exclusively from this single base station's communications signal, while other base stations operating on different frequencies do not interfere with the radar operations.
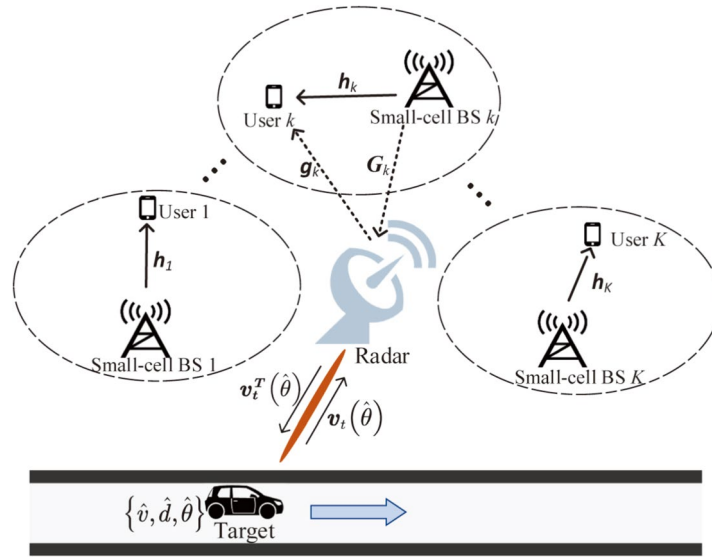
Fig. 1 A RCC system

Differing from the study in [25] and the conventional system where radar and communication systems share the same spectrum, we introduce a radar-communication coexistence system where the radar selectively re-uses the spectrum of small-cell BSs. Particularly, the radar chooses one of the small-cell BSs to re-use its spectrum. To realize the target detection and target tracking of radar, we propose a novel RCC frame structure which can be split into two stages, namely (1) radar target detection and (2) radar target tracking. At the detection stage, we propose a joint system design that fulfills the requirements of both radar and communication tasks and estimate parameters of the potential target. We aim to minimize the system power while simultaneously preserving radar detection performance and communication quality. At the tracking stage, we aim to maximize the radar sensing performance under a given power budget while ensuring communication quality. Furthermore, to mitigate the communication interference to the radar, a SIC-based algorithm for target parameter estimation is proposed. Compared with benchmark algorithms, the proposed algorithms show the superior performance.

3 System model

In this section, the model of the studied RCC system is introduced first. As shown in Fig. 1, we consider that there are K small-cell base stations which are covered by a co-located MIMO radar. Each small-cell BS is considered as a multiple-input single-output (MISO) communication system. To effectively manage inter-cell interference, we ensure that the spectrum assigned to each base station is orthogonal to that of its neighbors. This orthogonality is achieved through strategic frequency planning, where non-overlapping frequency bands are allocated to adjacent cells. The MIMO radar is a narrowband system, utilizing a uniform line array of half-wavelength spacing with M_T transmit antennas and M_R receive antennas. Each BS is equipped with N_T transmit antennas and serves one single-antenna user on each orthogonal channel [33, 34]. A single base station serving only one user seems less common in practical large-scale deployments.

However, the choice was strategically made to simplify the initial analysis and clearly demonstrate the fundamental interactions and spectrum sharing techniques between radar and communication systems. This scenario assumes a working bandwidth of 5MHz for all base stations. The radar is positioned alongside highways, covering a radius of several kilometers. The scenario involves one target that is a few kilometers away from the radar, and we have no prior knowledge of the target. We consider that the radar re-uses one of frequency bands occupied by the BS since the bandwidth of 5MHz is enough for the radar function. To track the target, we propose a detection-tracking framework comprising two stages: the detection stage, aimed at detecting the target, and the tracking stage, aimed at tracking the target.

3.1 Radar model

At the detection stage, due to the limited number of antennas, we divide the detection area into M directions to guarantee the detection performance, denoted by $\{\theta_m\}, \forall m \in \mathcal{M} \triangleq \{1, \ldots, M\}$, and it still works when the number of antennas increases [7]. Under a given pulse repetition interval (PRI), the radar transmits a train of L narrowband pulses. The space-time code matrix of the transmit signal is denoted by $\mathbf{S} = [\mathbf{s}_1, \ldots, \mathbf{s}_L] \in \mathbb{C}^{M_T \times L}$, where $\mathbf{s}_l \in \mathbb{C}^{M_T \times 1}$ is the vector of transmit signal at the l-th chirp.

Given that there is only one target within the radar's detection range and the ground and other clutter are relatively minor, the clutter can be approximated as Gaussian white noise. Therefore, the received signal from target in the direction θ_m at the radar can be expressed as

$$\mathbf{Y}_R = \underbrace{\alpha_m \mathbf{V}_m \tilde{\mathbf{S}}}_{\text{target echo}} + \underbrace{\sum_{k=1}^{K} \xi_k \mathbf{G}_k \mathbf{w}_k \mathbf{x}_k^T}_{\text{communication interference}} + \underbrace{\mathbf{N}}_{\text{noise}}, \tag{1}$$

where

- α_m represents the path loss in the system, which accounts for both the reflection coefficient and propagation loss. It is assumed to remain constant throughout a given period of radar pulse repetition.
- $\mathbf{V}_m = \mathbf{v}_r(\theta_m) \mathbf{v}_t^T(\theta_m)$, where $\mathbf{v}_t(\theta_m)$ and $\mathbf{v}_r(\theta_m)$ are the transmit and receive steering vectors of radar, defined as

$$\mathbf{v}_t(\theta_m) = \frac{1}{\sqrt{M_T}} \left[1, e^{j2\pi \triangle \frac{\sin \theta_m}{\lambda_0}}, \cdots, e^{j2\pi (M_T-1)\triangle \frac{\sin \theta_m}{\lambda_0}} \right]^T,$$

$$\mathbf{v}_r(\theta_m) = \frac{1}{\sqrt{M_R}} \left[1, e^{j2\pi \triangle \frac{\sin \theta_m}{\lambda_0}}, \cdots, e^{j2\pi (M_R-1)\triangle \frac{\sin \theta_m}{\lambda_0}} \right]^T,$$

where λ_0 is the wavelength and $\triangle$ is the space between antennas.

- ξ_k indicates whether the k-th BS shares the spectrum with the radar, which is a binary variable and satisfies that $\sum_{k=1}^{K} \xi_k = 1$.

- $\mathbf{G}_k \in \mathbb{C}^{M_R \times N_T}$ is the interference channel between the k-th BS and the radar.[1]
- $\mathbf{w}_k \in \mathbb{C}^{N_T \times 1}$ represents the transmission beamforming vector of the k-th BS.
- $\mathbf{x}_k = [x_{k,1}, x_{k,2}, \ldots, x_{k,L}]^T$ is the communication symbol vector transmitted from the k-th BS to the user, and the symbol stream $x_{k,l}$ is statistically independent with normalized power expectation.
- $\mathbf{N} \in \mathbb{C}^{M_R \times L}$ is the noise experienced at the radar receiver, and the element follows the Gaussian distribution, denoted as $\mathcal{CN}(0, \sigma_r^2)$.

Note that the target can be positioned as the (p, q)-th delay Doppler bin, and $\tilde{\mathbf{S}}$ is a delayed and Doppler-shifted counterpart of $\mathbf{S}$ [27],

$$\tilde{\mathbf{S}} = \left[\mathbf{S}\mathrm{diag}(\mathbf{d}_q), \mathbf{0}_{M_T \times P}\right]\mathbf{J}_p \in \mathbb{C}^{M_T \times (L+P)}, \tag{2}$$

where P represents the maximum delayed snapshots, and $\mathbf{d}_q$ is the Doppler frequency resulting from the movement of the target. It can be defined as

$$\mathbf{d}_q = [1, e^{j\frac{q}{Q}\Omega}, \ldots, e^{j\frac{q}{Q}\Omega(L-1)}]^T, \tag{3}$$

where $q \in \{-Q, \ldots, -1, 1, \ldots, Q\}$ represents the number of snapshots of the Doppler, Ω is the maximum number of detectable Doppler frequency, and Q is half of the maximum Doppler bins. Moreover, $\mathbf{J}_p$ is a matrix of the shift in the time domain, representing the round-trip time from the radar to the target, which is expressed as

$$\mathbf{J}_p = \begin{bmatrix} \mathbf{0}_{L \times p} & \mathbf{I}_{L+P-p} \\ \mathbf{0}_{p \times p} & \mathbf{0}_{(L+P-p) \times p} \end{bmatrix} \in \mathbb{R}^{(L+P) \times (L+P)}, \tag{4}$$

where $p \in \{1, \ldots, P\}$ is the number of snapshots of the delay.

After receiving the signal, the space-time receiver $\mathbf{u}_m$ is used to weight and combine the received raw signals to enhance signal quality or to extract specific signal features. $\mathbf{u}_{m,l}$ actually represents the effect of the radar receiver at the m-th receive antenna during time l. Thus $\mathbf{u}_m$ can be also regarded as a vector combination of L time segments, i.e., $\mathbf{u}_m = \left[\mathbf{u}_{m,1}^T, \cdots, \mathbf{u}_{m,L}^T\right]^T \in \mathbb{C}^{M_R L \times 1}$. Then, the corresponding signal-to-interference-plus-noise ratio (SINR) at the direction θ_m can be expressed as

$$\mathrm{SINR}^r(\theta_m) = \frac{\sum\limits_{l=1}^{L} \left|\mathbf{u}_{m,l}^H \alpha e^{j2\pi\frac{q}{Q}l}\mathbf{V}_m \mathbf{s}_l\right|^2}{\sum\limits_{k=1}^{K}\sum\limits_{l=1}^{L}\left|\xi_k\mathbf{u}_{m,l}^H\mathbf{G}_k\mathbf{w}_k\right|^2 + \sigma_r^2\sum\limits_{l=1}^{L}\left\|\mathbf{u}_{m,l}\right\|^2}. \tag{5}$$

3.2 Communication model

In the downlink communication system, each small-cell BS serves a single-antenna user. The received signal of the user associated with the k-th BS can be expressed as follows:

---

[1] To facilitate the joint beamforming design, we assume a centralized controller that connects all communication devices and the radar. This controller is capable of scheduling transmissions and acquiring channel information through advanced channel estimation algorithms. This enables seamless integration of radar and communication systems [35, 36].

$$y_{C,k,l} = \mathbf{h}_k^H \mathbf{w}_k x_{k,l} + \xi_k \mathbf{g}_k^H \mathbf{s}_l + n_{k,l}, \tag{6}$$

where $\mathbf{h}_k \in \mathcal{C}^{N_T \times 1}$ is the communication channel vector from the k-th BS to its user, $\mathbf{g}_k \in \mathbb{C}^{M_T \times 1}$ is the interference channel vector from the radar to the user, and $n_{k,l}$ follows the distribution $\mathcal{CN}(0, \sigma_c^2)$.

Then, the transmit power of the k-th BS can be written as $\|\mathbf{w}_k\|^2$ and the total power of the signal received by the corresponding user in one radar code-matrix length is

$$\mathbb{E}\left(\sum_{l=1}^{L} \left(y_{C,k}[l] \right)^H y_{C,k}[l] \right) = L\left| \mathbf{h}_k^H \mathbf{w}_k \right|^2 + \xi_k \sum_{l=1}^{L} \left| \mathbf{g}_k^H \mathbf{s}_l \right|^2 + L\sigma_c^2. \tag{7}$$

We use the average communication SINR as metric [6] for the communication quality, which can be expressed as

$$\text{SINR}_k^c = \frac{L\left| \mathbf{h}_k^H \mathbf{w}_k \right|^2}{\xi_k \sum_{l=1}^{L} \left| \mathbf{g}_k^H \mathbf{s}_l \right|^2 + L\sigma_c^2}. \tag{8}$$

Furthermore, we assume statistical independence between the communication signal and the radar waveform.

3.3 Detection and tracking framework

Regarding the scenario where the radar and a small-cell BS share the same spectrum and the target keeps moving, we propose a frame structure that can be divided into the following two stages to achieve radar target detection and tracking while maintaining communication quality.

3.3.1 Radar target detection

At this stage, the radar lacks prior information about the target and must conduct a comprehensive search across the entire space to identify potential targets. The radar chooses one small-cell BS to re-use its spectrum and sends an omnidirectional signal to detect the potential target. Subsequently, the angle of the target, as well as the delay and Doppler parameters, is then estimated. After that, the system effectively searches for the radar target while maintaining the desired communication quality of the coexisting small-cell base station operating in the shared spectrum. The joint design of the detection stage (JD-DS) and the parameter estimation (PE) for the target are shown in Fig. 2. The specific details of JD-DS can be found in Sect. 5. Details of parameter estimation are given in Sect. 4.

3.3.2 Radar target tracking

After the detection stage, the system obtains the initial parameters of the target. At the tracking stage, the time period is divided into multiple smaller time slots with a length of ΔT and denote $\left\{ \tilde{\theta}_t, \tilde{d}_t, \tilde{v}_t \right\}$ as the predicted parameters at the t-th epoch. The radar periodically transmits signals to obtain the state information of the target, thereby realizing the tracking for the target. At this stage, we maximize the sensing performance of the radar while maintaining the communication quality of the selected small-cell BS under a transmit
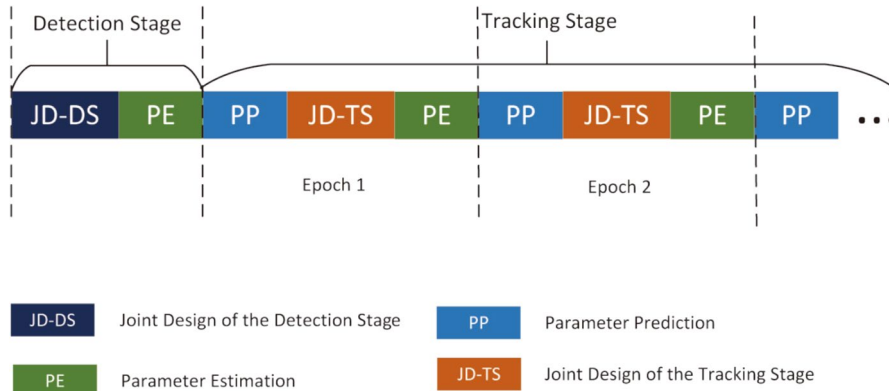
Mao *et al. J Wireless Com Network*   (2024) 2024:56

Page 8 of 28

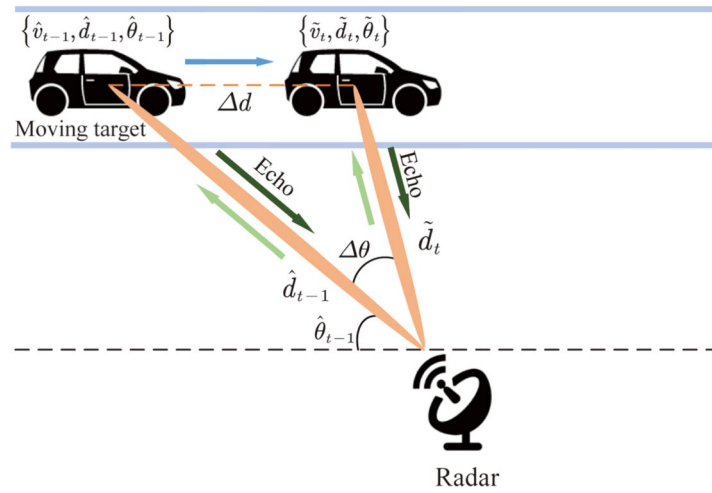**Fig. 2** Frame structure of the RCC system

Fig. 3 Target state evolution model

power budget. However, to jointly design the system, it is imperative to predict the parameters of the target at the current moment. Before that, the radar has obtained the parameters at the $(t-1)$-th epoch by PE, which are expressed as $\left\{\hat{\theta}_{t-1}, \hat{d}_{t-1}, \hat{v}_{t-1}\right\}$. According to the state evolution model [28], as shown in Fig. 3, we have

$$\begin{cases} \tilde{d}_t^{\,2} = \hat{d}_{t-1}^2 + \Delta d^2 - 2\hat{d}_{t-1}\Delta d \cos\hat{\theta}_{t-1}, \\ \frac{\Delta d}{\sin\Delta\theta} = \frac{\tilde{d}_t}{\sin\hat{\theta}_{t-1}}, \end{cases} \tag{9}$$

where $\Delta d = \hat{v}_{t-1}\Delta T$ and $\Delta\theta = \tilde{\theta}_t - \hat{\theta}_{t-1}$. We assume that the target keeps moving at an approximately constant speed within ΔT. Therefore, we can predict the target parameters. The state evolution model is summarized as

$$\begin{cases} \tilde{\theta}_t = \hat{\theta}_{t-1} + \hat{d}_{t-1}^{-1}\hat{v}_{t-1}\Delta T \sin\hat{\theta}_{t-1} + \omega_\theta, \\ \tilde{d}_t = \hat{d}_{t-1} - \hat{v}_{t-1}\Delta T \cos\hat{\theta}_{t-1} + \omega_d, \\ \tilde{v}_t = \hat{v}_{t-1} + \omega_v, \end{cases} \tag{10}$$

where $\omega_\theta, \omega_d, \omega_v$ are the corresponding noises, which can be assumed to follow Gaussian distribution with the mean value of 0 and the variance of $\sigma_\theta^2, \sigma_d^2, \sigma_v^2$, respectively.

The parameter prediction (PP) is shown in Fig. 2. After obtaining the predicted parameters of the target at the current moment, we carry out the joint design of the tracking stage (JS-TS) as shown in Fig. 2. Then, we estimate the real parameters of the target at the current moment.

At the tracking stage, the joint design of the radar-communication system performance maximization is accomplished by JS-TS, with the reference parameters of the target provided by PP. The real parameters of the target are subsequently estimated by PE using the received signal. The state information of the target is iteratively updated through a repetition of the PP, JS-TS, and PE, ultimately achieving the target tracking.

4 Parameter estimation

In this section, we estimate the angle, delay, and Doppler of the radar target from the received signal. Firstly, the classical multiple signal classification (MUSIC) algorithm [37] is used to estimate the angle of the target. Secondly, a SIC-based parameter estimation algorithm is proposed to accurately estimate the delay and Doppler frequency of the target while eliminating the interference from the communication system in the received signal. These estimated parameters are then used to deduce the distance and speed of the target, respectively.

4.1 Delay and Doppler estimation

With the estimated angle, the next step is to estimate the delay bin p and the Doppler bin q. Here we propose a SIC-based parameter estimation algorithm, which iteratively extracts the target echo and the communication interference from the received signal to improve the estimation accuracy.

Algorithm 1 SIC-based parameter estimation algorithm.

1: Initialize the iteration number $i = 0$, the maximum number of iterations $I_{\max}^e$, and the tolerance of accuracy ϵ_e.
2: **while** the gap between two consecutive iterations is higher than ϵ_e and $i < I_{\max}^e$. **do**
3:     Obtain $\hat{p}, \hat{q}$ in (13);
4:     Obtain $\hat{\mathbf{x}}$ in (14);
5:     Obtain $\hat{\mathbf{N}}$ in (16);
6:     Obtain $\mathbf{Y}_r'$ in (17);
7:     $i = i + 1$;
8: **end while**

4.1.1 Initial estimation

With the estimated AOA, θ_m, the reference signal in the (p, q)-th delay Doppler bin is vectorized as

$$\mathbf{y}_{\text{ref,p,q}} = \text{vec}\left(\mathbf{v}_r(\theta_m)\mathbf{v}_t^T(\theta_m)\left[\mathbf{S}\text{diag}(\mathbf{d}_q),\mathbf{0}_{M_T \times P}\right]\mathbf{J}_p\right), \tag{11}$$

where $\mathbf{d}_q$ and $\mathbf{J}_p$ are defined by (3) and (4), representing the p-th range bin and the q-th Doppler bin, respectively. We also vectorize the received signal, denoted by $\tilde{\mathbf{y}}_R = \text{vec}(\mathbf{Y}_R)$. Since we have

$$\left|\mathbf{y}_{\text{ref,p,q}}^H \mathbf{y}_{\text{ref,p',q'}}\right| \leq \left|\mathbf{y}_{\text{ref,p,q}}^H \mathbf{y}_{\text{ref,p,q}}\right|, \quad \forall p, q \neq p', q'. \tag{12}$$

We can use the matched filter (MF) algorithm to obtain the estimated parameters $\{\hat{p}, \hat{q}\}$ as follows

$$\{\hat{p}, \hat{q}\} = \arg\max_{\{p,q\}} \left|\tilde{\mathbf{y}}_R^H \mathbf{y}_{\text{ref},p,q}\right|. \tag{13}$$

4.1.2 Iterative parameter refinement

In the above process, the parameters of the radar target are estimated. However, the accuracy of these estimates is seriously affected by the interference from the communication system. To improve the accuracy of the parameter estimation, we propose a SIC-based estimation algorithm that iteratively corrects the estimated target parameters by extracting the target echo and communication interference from the received signal.

First, we use the delay bin p, and Doppler bin q, obtained in (13) to reconstruct the target echo $\mathbf{Y}_r$. Then, we subtract this part from the received signal $\mathbf{Y}_R$, and obtain the residual signal denoted as $\mathbf{Y}_{\text{res}}$. We regard $\mathbf{Y}_{\text{res}}$ as interference from the communication system to the radar. Then, we can use the known communication and interference channel information to demodulate the communication transmit signal. With minimizing the mean squared error, we can demodulate the communication signal $\hat{\mathbf{x}}_k$ as

$$\hat{\mathbf{x}}_k = \arg\min_{\mathbf{x}_k} \left\|\mathbf{Y}_{\text{res}} - \mathbf{G}_k \mathbf{w}_k \mathbf{x}_k^T\right\|^2. \tag{14}$$

Using the least squares method (LSM), we can estimate the communication signal as

$$\hat{\mathbf{x}}_k^T = \left((\mathbf{G}_k \mathbf{w}_k)^H (\mathbf{G}_k \mathbf{w}_k)\right)^{-1} (\mathbf{G}_k \mathbf{w}_k)^H \mathbf{Y}_{\text{res}}. \tag{15}$$

After the demodulation of the communication signal, we use it to reconstruct the communication interference denoted as $\mathbf{Y}_{\text{intf}}$. Then, we can write the new residual signal as

$$\hat{\mathbf{N}} = \mathbf{Y}_R - \mathbf{Y}_r - \mathbf{Y}_{\text{intf}}. \tag{16}$$

This part of residual signal is treated as background noise.

To mitigate the impact of estimation errors and energy leakage in the residual signal, we propose to use the reconstructed target echo and the background noise to formulate a new target echo. This is motivated by the fact that the previous reconstruction of the target echo may not be the same as the actual echo due to estimation errors. The new target echo is obtained through subtraction of the estimated communication signal from the current received signal. This process is repeated iteratively to further improve the accuracy of the estimation.

$$\mathbf{Y}_{\mathrm{r}}' = \mathbf{Y}_{\mathrm{r}}(\hat{p}, \hat{q}) + \hat{\mathbf{N}}, \tag{17}$$

where $\mathbf{Y}_{\mathrm{r}}(\hat{p}, \hat{q})$ represents the target echo reconstructed by the latest estimated parameters $(\hat{p}, \hat{q})$ from (13). Now we have a better target echo $\mathbf{Y}_{\mathrm{r}}'$, which contains less interference than the target echo estimated previously, $\mathbf{Y}_{\mathrm{r}}$. With the refined radar signal, we can estimate better target state information by feeding it back to (13), in which case we start a new round estimation process. The above steps of reconstruction and re-estimation are iterated until the gap between two consecutive iterations is smaller than the given threshold, denoted by ϵ_e or the number of iterations goes beyond its upper limitation, denoted by $I_{\max}^e$. Note that ϵ_e and $I_{\max}^e$ can be set according to different accuracy requirements.

5 Radar target detection

In this section, we first present the generation method of radar omnidirectional signal under a given transmit power budget to detect the potential target in the whole space. Next, we propose a method of radar spectrum selection and joint system design while maintaining radar detection performance and communication quality of the BS whose spectrum is shared. To address the problem, we propose a PDD-based algorithm for the detection stage (PA-DS). Specifically, we employ a traversal algorithm to explore the joint design of the system for each base station when the radar spectrum is shared. For solving this optimization problem, we propose a PDD-based algorithm.

5.1 Problem formulation

In this stage, we have no prior information about the target; a common method is to transmit equivalent power at each angle by an omnidirectional waveform denoted by $\mathbf{S}_0 \in \mathbb{C}^{M_\mathrm{T} \times L}$. To do so, we adopt a commonly used MIMO radar waveform that is the orthogonal linear frequency modulation (LFM) signals. According to [38], on the m_t-th antenna at the l-th chirp, the (m_t, l)-th entry of the orthogonal LFM waveform matrix under unit power can be expressed as

$$\mathbf{S}_0(m_\mathrm{t}, l) = \sqrt{\frac{1}{M_\mathrm{T}}} \exp\left(\left(\frac{j2\pi m_\mathrm{t}(l-1)}{L}\right)\left(\frac{j\pi(l-1)^2}{L}\right)\right). \tag{18}$$

And its covariance matrix satisfies

$$\mathbf{R}_{\mathbf{S}_0} = \frac{1}{L}\mathbf{S}_0\mathbf{S}_0^H = \frac{1}{M_\mathrm{T}}\mathbf{I}_{M_\mathrm{T}}. \tag{19}$$

In this case, the spatial beampattern is

$$d(\theta) = \mathbf{v}_\mathrm{r}^T(\theta)\mathbf{R}_{\mathbf{S}_0}\mathbf{v}_\mathrm{t}^*(\theta) = 1, \forall \theta, \tag{20}$$

which is an omnidirectional beampattern. As the transmit power is denoted by P_T, the transmit waveform matrix can be expressed as $p_\mathrm{T}\mathbf{S}_0$ with $P_\mathrm{T} = p_\mathrm{T}^2$. In this stage, the radar periodically transmits signals to detect potential targets, while K small-cell BSs are all in downlink communication. Our goal is to achieve the minimization of the system's total transmit power by selecting a BS for spectrum sharing and designing a joint

radar-communication system, while ensuring the quality of downlink communication and radar detection performance. Since radar SINR is positively correlated with radar performance and is used in many studies [7, 39], we adopt this metric in our approach. Hence, we formulate the optimization problem as follows,

$$\min_{\{\mathbf{u}_m, \xi_k, p_{\mathrm{T}}, \mathbf{w}_k\}} \quad \sum_{k=1}^{K} \|\mathbf{w}_k\|^2 + \frac{p_{\mathrm{T}}^2}{L}, \tag{21a}$$

$$\text{s.t.} \quad \mathrm{SINR}_k^{\mathrm{c}} \geq \gamma^{\mathrm{c}}, \forall k, \tag{21b}$$

$$\mathrm{SINR}^{\mathrm{r}}(\theta_m) \geq \gamma^{\mathrm{r}}, \forall m, \tag{21c}$$

$$\sum_{k=1}^{K} \xi_k = 1, \tag{21d}$$

$$\xi_k \in \{0, 1\}, \tag{21e}$$

where (21b) ensures that the communication SINR of each small-cell BS is not less than the lower bound γ^{c}, γ^{r} is the threshold of radar SINR, and (21c) ensures the minimum detection probability of the radar at each detection direction. To account for practical considerations, we normalize the optimal receiver vector and there is no power constraint for $\mathbf{u}_{m,l}$. It is obvious that we only need to consider the co-design between the radar and the small-cell BS that shares the spectrum with the radar. Since the number of small-cell BSs within the radar coverage is limited, the problem in (21) can be simplified by traversing ξ_k. By assuming that the $\hat{k}$-th BS is selected to share the spectrum with the radar. As for other BSs who are not selected, the transmit vector can be easily derived as

$$\mathbf{w}_k = \frac{\gamma^c \sigma_{\mathrm{c}}^2}{\|\mathbf{h}_k\|^2} \mathbf{h}_k, \ \forall k \neq \hat{k}. \tag{22}$$

The subproblem to the $\hat{k}$-th BS is formulated as

$$\min_{\{p_{\mathrm{T}}, \mathbf{u}_m, \mathbf{w}_{\hat{k}}\}} \quad \left\| \mathbf{w}_{\hat{k}} \right\|^2 + \frac{p_{\mathrm{T}}^2}{L}, \tag{23a}$$

$$\text{s.t.} \quad \frac{L \left| \mathbf{h}_{\hat{k}}^H \mathbf{w}_{\hat{k}} \right|^2}{p_{\mathrm{T}}^2 \sum\limits_{l=1}^{L} \left| \mathbf{g}_{\hat{k}}^H \mathbf{s}_{0,l} \right|^2 + L \sigma_{\mathrm{c}}^2} \geq \gamma^{\mathrm{c}}, \tag{23b}$$

$$\frac{p_{\mathrm{T}}^2 \sum\limits_{l=1}^{L} \left| \mathbf{u}_{m,l}^H \alpha e^{j2\pi \frac{q}{Q} l} \mathbf{V}_m \mathbf{s}_{0,l} \right|^2}{\sum\limits_{l=1}^{L} \left| \mathbf{u}_{m,l}^H \mathbf{G}_{\hat{k}} \mathbf{w}_{\hat{k}} \right|^2 + \sigma_{\mathrm{r}}^2 \sum\limits_{l=1}^{L} \left\| \mathbf{u}_{m,l} \right\|^2} \geq \gamma^{\mathrm{r}}, \forall m. \tag{23c}$$

Due to the intricate coupling and non-convex constraints, solving the aforementioned problem poses a considerable challenge. In the subsequent subsection, we propose a PDD-based algorithm featuring a double-layer loop, which effectively transforms and resolves the original problem.

5.2 Algorithm design

5.2.1 PDD framework

Define an optimization problem as $\mathcal{P}$

$$\mathcal{P} : \min_{\boldsymbol{x} \in \mathcal{X}} \quad f(\boldsymbol{x}), \tag{24a}$$

$$\text{s.t.} \quad \boldsymbol{h}(\boldsymbol{x}) = 0, \tag{24b}$$

$$\boldsymbol{g}(\boldsymbol{x}) \leq 0, \tag{24c}$$

where $f(\boldsymbol{x})$ is the continuously differentiable objective function with respect to the vector $\mathbf{x}$, and $\boldsymbol{h}(\boldsymbol{x})$ and $\boldsymbol{g}(\boldsymbol{x})$ are the continuously differentiable functions. The augmented Lagrangian (AL) problem, $\mathcal{P}\left(\rho^{(i)}, \boldsymbol{\lambda}^{(i)}\right)$, at the i-th iteration is given by

$$\min_{\boldsymbol{x} \in \mathcal{X}} \quad \mathcal{L}^{(i)}(\boldsymbol{x}) \triangleq f(\boldsymbol{x}) + \frac{1}{2\rho^{(i)}} \left\| \boldsymbol{h}(\boldsymbol{x}) + \rho^{(i)} \boldsymbol{\lambda}^{(i)} \right\|^2, \tag{25a}$$

$$\text{s.t.} \quad \boldsymbol{g}(\boldsymbol{x}) \leq 0, \tag{25b}$$

where $\mathcal{L}^{(i)}(\boldsymbol{x})$ represents the transformed AL problem with penalty factor and dual factor in the i-th outer loop. In the inner loop, the AL problem is solved. In the outer loop, we update the penalty factor $\rho^{(i)}$ or the dual factor $\lambda^{(i)}$. The PDD method dynamically alternates between AL and penalty approaches. This adaptive mechanism aims to identify an optimal penalty parameter that ensures the convergence of the AL method. According to [40], when the penalty factor $\rho^{(i)} \to 0$, the AL problem $\mathcal{P}\left(\rho^{(i)}, \boldsymbol{\lambda}^{(i)}\right)$ is equivalent to the original problem. The convergence of the PDD algorithm has been proved in [41, 42], and it finally converges to a stationary point of $\boldsymbol{x}^{(i)}$.

5.2.2 Problem solving

Since the constraints in problem (23) are highly coupled, it is difficult to apply the PDD framework. Through the introduction of auxiliary variables, we transform the problem into a more tractable form, enabling us to derive closed-form solutions for the subproblems. To solve the AL problem in the inner loop, we propose a concave–convex procedure (CCCP)-based algorithm [43]. We introduce new auxiliary variables $z, x_{m,l}, y_{m,l}, \forall m, l$,

$$z = \mathbf{h}_{\hat{k}}^H \mathbf{w}_{\hat{k}}, \tag{26a}$$

$$x_{m,l} = p_{\mathrm{T}} \mathbf{u}_{m,l}^H \mathbf{a}_{m,l}, \forall m, l, \tag{26b}$$

Mao *et al. J Wireless Com Network*   (2024) 2024:56

Page 14 of 28

$$y_{m,l} = \mathbf{u}_{m,l}^H \mathbf{G}_{\hat{k}} \mathbf{w}_{\hat{k}}, \forall m, l, \tag{26c}$$

where $\mathbf{a}_{m,l} = \alpha e^{j 2\pi \frac{q}{Q} l} \mathbf{V}_m \mathbf{s}_{0,l}$. Constraints (23b) and (23c) can be rewritten as

$$\gamma^{\mathrm{c}} \left(p_{\mathrm{T}}^2 \sum_{l=1}^{L} \left| \mathbf{g}_{\hat{k}}^H \mathbf{s}_{0,l} \right|^2 + L \sigma_{\mathrm{c}}^2 \right) - L |z|^2 \le 0, \tag{27a}$$

$$\gamma^{\mathrm{r}} \left(\sigma_{\mathrm{r}}^2 \sum_{l=1}^{L} \|\mathbf{u}_{m,l}\|^2 + \sum_{l=1}^{L} |y_{m,l}|^2 \right) - \sum_{l=1}^{L} |x_{m,l}|^2 \le 0, \forall m. \tag{27b}$$

With AL multipliers $\Gamma_1 = \{\lambda_{1,m,l}, \lambda_{2,m,l}, \lambda_3, \forall m, l\}$, we introduce (26a), (26b), and (26c) into the objective function, and an alternative AL problem in the inner loop can be formulated as

$$\min_{\mathbb{X}_1} \left\| \mathbf{w}_{\hat{k}} \right\|^2 + \frac{p_{\mathrm{T}}^2}{L} + \frac{1}{2\rho} \left| z - \mathbf{h}_{\hat{k}}^H \mathbf{w}_{\hat{k}} + \rho \lambda_3 \right|^2$$

$$+ \frac{1}{2\rho} \sum_{m=1}^{M} \sum_{l=1}^{L} \left| x_{m,l} - p_{\mathrm{T}} \mathbf{u}_{m,l}^H \mathbf{a}_{m,l} + \rho \lambda_{1,m,l} \right|^2 \tag{28a}$$

$$+ \frac{1}{2\rho} \sum_{m=1}^{M} \sum_{l=1}^{L} \left| y_{m,l} - \mathbf{u}_{m,l}^H \mathbf{G}_{\hat{k}} \mathbf{w}_{\hat{k}} + \rho \lambda_{2,m,l} \right|^2,$$

$$\text{s.t. } \gamma^{\mathrm{c}} \left(p_{\mathrm{T}}^2 \sum_{l=1}^{L} \left| \mathbf{g}_{\hat{k}}^H \mathbf{s}_{0,l} \right|^2 + L \sigma_{\mathrm{c}}^2 \right) - L |z|^2 \le 0, \tag{28b}$$

$$\gamma^{\mathrm{r}} \left(\sigma_{\mathrm{r}}^2 \sum_{l=1}^{L} \|\mathbf{u}_{m,l}\|^2 + \sum_{l=1}^{L} |y_{m,l}|^2 \right) - \sum_{l=1}^{L} |x_{m,l}|^2 \le 0, \forall m, \tag{28c}$$

where $\mathbb{X}_1 = \left\{ p_{\mathrm{T}}, \mathbf{w}_{\hat{k}}, z, \mathbf{u}_{m,l}, x_{m,l}, y_{m,l} \right\}$ is the set of optimization variables. As proved in [41, 42], the problem in (28) is equivalent to the original problem in (21) when $\rho \to 0$. Moreover, by utilizing the first-order Taylor expansion, $z, x_{m,l}$ of the constraints (28b), (28c) in the j-th iteration can be approximated with

$$|z|^2 \approx - \left| z^{(j)} \right|^2 + 2\Re \left(\left(z^{(j)} \right)^* z \right), \tag{29a}$$

$$|x_{m,l}|^2 \approx - \left| x_{m,l}^{(j)} \right|^2 + 2\Re \left(\left(x_{m,l}^{(j)} \right)^* x_{m,l} \right). \tag{29b}$$

Then, constraint (28b) and (28c) can be approximated with

$$\gamma^{\mathrm{c}} \left(p_{\mathrm{T}}^2 \sum_{l=1}^{L} \left| \mathbf{g}_{\hat{k}}^H \mathbf{s}_{0,l} \right|^2 + L \sigma_{\mathrm{c}}^2 \right) + L \left| z^{(j)} \right|^2 - 2L \Re \left(\left(z^{(j)} \right)^* z \right) \le 0, \tag{30}$$

$$\gamma^{\mathrm{r}} \left(\sigma_{\mathrm{r}}^2 \sum_{l=1}^{L} \left\| \mathbf{u}_{m,l} \right\|^2 + \sum_{l=1}^{L} \left| y_{m,l} \right|^2 \right) + \sum_{l=1}^{L} \left| x_{m,l}^{(j)} \right|^2 - \sum_{l=1}^{L} 2 \Re \left(\left(x_{m,l}^{(j)} \right)^* x_{m,l} \right) \le 0, \forall m. \tag{31}$$

Thus, problem (28) is reformulated as

$$\min_{\mathbb{X}_1} \frac{1}{2\rho} \sum_{m=1}^{M} \sum_{l=1}^{L} \left| x_{m,l} - p \mathbf{u}_{m,l}^H \mathbf{a}_{m,l} + \rho \lambda_{1,m,l} \right|^2$$

$$+ \frac{1}{2\rho} \sum_{m=1}^{M} \sum_{l=1}^{L} \left| y_{m,l} - \mathbf{u}_{m,l}^H \mathbf{G}_{\hat{k}} \mathbf{w}_{\hat{k}} + \rho \lambda_{2,m,l} \right|^2 \tag{32a}$$

$$+ \left\| \mathbf{w}_{\hat{k}} \right\|^2 + \frac{p_{\mathrm{T}}^2}{L} + \frac{1}{2\rho} \left| z - \mathbf{h}_{\hat{k}}^H \mathbf{w}_{\hat{k}} + \rho \lambda_3 \right|^2,$$

s.t. (30) and (31),

which can be proved as a convex problem. To derive the closed-form solution and reduce time complexity, we can utilize the block coordinate descent (BCD) algorithm [40] to solve the above problem. The variables are divided into two blocks, and two subproblems are proposed. Specifically, the details are shown as follows.

In **Step 1**, we optimize $\left\{ p_{\mathrm{T}}, \mathbf{w}_{\hat{k}}, z \right\}$ while fixing other variables, with respect to the following subproblem

$$\min_{\left\{ p_{\mathrm{T}}, \mathbf{w}_{\hat{k}}, z \right\}} \frac{1}{2\rho} \sum_{m=1}^{M} \sum_{l=1}^{L} \left| x_{m,l} - p_{\mathrm{T}} \mathbf{u}_{m,l}^H \mathbf{a}_{m,l} + \rho \lambda_{1,m,l} \right|^2$$

$$+ \frac{1}{2\rho} \sum_{m=1}^{M} \sum_{l=1}^{L} \left| y_{m,l} - \mathbf{u}_{m,l}^H \mathbf{G}_{\hat{k}} \mathbf{w}_{\hat{k}} + \rho \lambda_{2,m,l} \right|^2 \tag{33a}$$

$$+ \frac{1}{2\rho} \left| z - \mathbf{h}_{\hat{k}}^H \mathbf{w}_{\hat{k}} + \rho \lambda_3 \right|^2 + \left\| \mathbf{w}_{\hat{k}} \right\|^2 + \frac{p_{\mathrm{T}}^2}{L},$$

s.t. (30).

The Lagrange multiplier method is applied to solve the problem above, and $\left\{ p_{\mathrm{T}}^{\star}, \mathbf{w}_{\hat{k}}^{\star}, z^{\star} \right\}$ are denoted as the optimal solution. The detailed derivation is omitted for brevity.

In **Step 2**, we optimize $\left\{ \mathbf{u}_{m,l}, x_{m,l}, y_{m,l} \right\}$ in parallel with the $\left\{ p_{\mathrm{T}}^{\star}, \mathbf{w}_{\hat{k}}^{\star}, z^{\star} \right\}$ derived in step 1. The subproblem is formulated as

$$\min_{\left\{ \mathbf{u}_{m,l}, x_{m,l}, y_{m,l} \right\}} \sum_{l=1}^{L} \left| x_{m,l} - p_{\mathrm{T}}^{\star} \mathbf{u}_{m,l}^H \mathbf{a}_{m,l} + \rho \lambda_{1,m,l} \right|^2$$

$$+ \sum_{l=1}^{L} \left| y_{m,l} - \mathbf{u}_{m,l}^H \mathbf{G}_{\hat{k}} \mathbf{w}_{\hat{k}}^{\star} + \rho \lambda_{2,m,l} \right|^2, \tag{34a}$$

s.t. (31).

The Lagrange multiplier method is applied to solve the problem and $\left\{ \mathbf{u}_{m,l}^{\star}, x_{m,l}^{\star}, y_{m,l}^{\star} \right\}$ are denoted as the optimal solution. The detailed derivation is omitted for brevity.

With the transformation and the corresponding solutions of subproblems, the proposed CCCP-based algorithm to solve the AL problem is summarized in Algorithm 2.

Algorithm 2 Proposed CCCP-based algorithm in the inner loop.

1: Set variables $\mathbb{X}_1 = \left\{ p_T, \mathbf{w}_{\hat{k}}, z, \mathbf{u}_{m,l}, x_{m,l}, y_{m,l} \right\}$.
2: Initialize the iteration number $i = 0$, the tolerance of accuracy ϵ_1, and the maximum number of iterations $I_{\max}$.
3: **while** $i < I_{\max}$ and the difference between consecutive values of the objective function is higher than ϵ_1. **do**
4:     Update $p_T, \mathbf{w}_{\hat{k}}, z$ in **Step 1**;
5:     Update $\mathbf{u}_{m,l}, x_{m,l}, y_{m,l}$ in **Step 2**;
6:     $i = i + 1$;
7: **end while**

Recall that we aim to solve the original problem in (21) by the PDD framework, and we have solved the AL problem in the inner loop by utilizing the CCCP-based algorithm. In the outer loop, the dual variables $\lambda_{1,m,l}, \lambda_{2,m,l}, \lambda_3, \forall m$ or the penalty factor ρ are updated. The dual variables at the i-th iteration can be updated as

$$\lambda_{1,m,l}^{(i)} = \lambda_{1,m,l}^{(i-1)} + \frac{1}{\rho^{(i-1)}} \left(x_{m,l}^{(i-1)} - p_{\mathrm{T}}^{(i-1)} (\mathbf{u}_{m,l}^{(i-1)})^H \mathbf{a}_{m,l}^{(i-1)} \right), \forall m, l, \tag{35a}$$

$$\lambda_{2,m,l}^{(i)} = \lambda_{2,m,l}^{(i-1)} + \frac{1}{\rho^{(i-1)}} \left(y_{m,l}^{(i-1)} - (\mathbf{u}_{m,l}^{(i-1)})^H \mathbf{G}_{\hat{k}} \mathbf{w}_{\hat{k}}^{(i-1)} \right), \forall m, l, \tag{35b}$$

$$\lambda_3^{(i)} = \lambda_3^{(i-1)} + \frac{1}{\rho^{(i-1)}} \left(z^{(i-1)} - \mathbf{h}_{\hat{k}}^H \mathbf{w}_{\hat{k}}^{(i-1)} \right). \tag{35c}$$

The indicator of constraint violation is defined as

$$h(\mathbb{X}_1) = \max \left\{ \left| z - \mathbf{h}_{\hat{k}}^H \mathbf{w}_{\hat{k}} \right|, \max \left\{ \left| x_{m,l} - p_{\mathrm{T}} \mathbf{u}_{m,l}^H \mathbf{a}_{m,l} \right|, \left| y_{m,l} - \mathbf{u}_{m,l}^H \mathbf{G}_{\hat{k}} \mathbf{w}_{\hat{k}} \right|, \forall m, l \right\} \right\}. \tag{36}$$

According to [41], the convergence of the proposed algorithm to a stationary point of the original problem can be proved when $h(\mathbb{X}_1) \to 0$.

The computational complexity of the proposed PDD-based algorithm is derived as follows. We denote $I_{\max}$ and $I_{\max}^o$ as the required numbers of iteration in the inner loop and outer loop, respectively. At each iteration of the inner loop, the computational complexities of two steps are $\mathcal{O}(N_{\mathrm{T}}^2 (\mathrm{ML} M_{\mathrm{R}} + 1) + \log \frac{I_0}{\varepsilon})$ and $\mathcal{O}(\mathrm{ML}(M_{\mathrm{R}}^2 (N_{\mathrm{T}} + 1) + \log \frac{I_0}{\varepsilon}))$, respectively, where I_0 is the size of initial range and ε is the tolerance of accuracy. Then, the computational complexity under a given ξ_k is obtained. Therefore, we propose the PA-DS algorithm which is shown in Fig. 4 to solve the problem in (21) with traversal algorithm. To be specific, we solve the subproblem in (23) by using the PDD-based algorithm with given BS selection and then choose the minimal power among the power under different BS selection. Since the number of base stations is limited and relatively small, the computational complexity of sequentially traversing the shared base stations is controllable. Overall, the total complexity of the PA-DS algorithm is summarized as
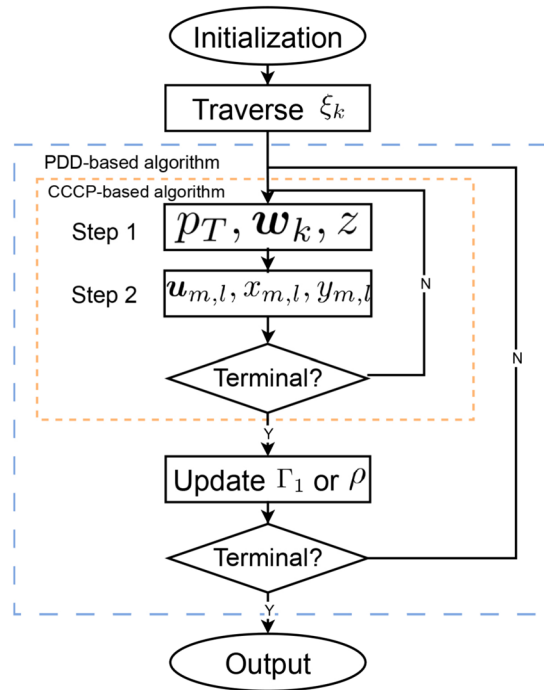
Fig. 4 The structure of the proposed PA-DS algorithm

$$\mathcal{O}(KI^o_{\max}I_{\max}(\mathrm{ML}M_R N_{\mathrm{T}}(M_R + N_{\mathrm{T}}) + \mathrm{ML}\log\frac{I_0}{\varepsilon})). \tag{37}$$

6 Radar target tracking

In this section, we aim to implement target tracking after the detection stage. To achieve this goal, we propose a novel joint design of the radar-communication system, which takes into account both the target tracking and downlink communication. In contrast to the detection stage, we seek to design the radar transmit waveform $\mathbf{S}_{\mathrm{T}} = [\mathbf{s}_{t,1},\cdots,\mathbf{s}_{t,L}] \in \mathbb{C}^{M_T \times L}$. With the predicted parameters at the t-th epoch, $\left\{\tilde{\theta}_t, \tilde{d}_t, \tilde{v}_t\right\}$, the delay Doppler bin $\{p_{\mathrm{T}}, q_{\mathrm{T}}\}$ can be derived, and the received signal at the t-th epoch on the radar can be defined as

$$\mathbf{Y}_{R,t} = \alpha_{\mathrm{t}}\mathbf{V}_t\tilde{\mathbf{S}}_{\mathrm{t}} + \sum_{k=1}^{K}\xi_{t,k}\mathbf{G}_k\mathbf{w}_{t,k}\mathbf{x}_k^T + \mathbf{N}_{\mathrm{t}}, \tag{38}$$

where $\mathbf{V}_t = \mathbf{v}_r(\tilde{\theta}_t)\mathbf{v}_t^T(\tilde{\theta}_t)$. $\alpha_{\mathrm{t}}, \tilde{\mathbf{S}}_{\mathrm{t}}, \mathbf{w}_{t,k}, \xi_{t,k}$, and $\mathbf{N}_{\mathrm{t}}$ are the path loss which are similar to (1), Doppler-shifted counterpart of $\mathbf{S}_{\mathrm{t}}$, the BS transmit vector, the BS selection indicator, and the noise at the t-th epoch, respectively. With the receiver $\mathbf{u}_{\mathrm{t}} = \left[\mathbf{u}_{t,1}^T,\cdots,\mathbf{u}_{t,L}^T\right]^T \in \mathbb{C}^{M_R L \times 1}$, the radar SINR at the t-th epoch can be expressed as

$$\text{SINR}^{\text{r}}(\theta_{\text{t}}) = \frac{\sum\limits_{l=1}^{L} \left| \mathbf{u}_{t,l}^{H} \alpha_{\text{t}} e^{j2\pi \frac{q_{\text{t}}}{Q} l} \mathbf{V}_t \mathbf{s}_{t,l} \right|^2}{\sum\limits_{k=1}^{K} \sum\limits_{l=1}^{L} \xi_{t,k} \left| \mathbf{u}_{t,l}^{H} \mathbf{G}_k \mathbf{w}_{t,k} \right|^2 + \sigma_{\text{r}}^2 \sum\limits_{l=1}^{L} \left\| \mathbf{u}_{t,l} \right\|^2}. \tag{39}$$

6.1 Problem formulation

At the tracking stage, our objective is to maximize sensing accuracy while meeting the communication requirement of the BS. The radar's sensing performance is influenced by the SINR, while the downlink transmission quality relies on the communication SINR. Accordingly, we formulate the optimization problem in the t-th epoch as follows,

$$\max_{\{\mathbf{u}_t, \xi_{t,k}, \mathbf{S}_t, \mathbf{w}_{t,k}\}} \quad \text{SINR}^{\text{r}}(\theta_{\text{t}}), \tag{40a}$$

$$\text{s.t.} \quad \text{SINR}_k^{\text{c}} \geq \gamma^{\text{c}}, \forall k, \tag{40b}$$

$$\frac{1}{L} \|\mathbf{S}_{\text{t}}\|^2 \leq P^{\text{r}}, \tag{40c}$$

$$\left\| \mathbf{w}_{t,k} \right\|^2 \leq P^{\text{c}}, \forall k, \tag{40d}$$

$$\sum_{k=1}^{K} \xi_{t,k} = 1, \tag{40e}$$

$$\xi_{t,k} \in \{0, 1\}, \tag{40f}$$

where (40b) indicates that each BS must meet the minimum required communication SINR, γ^{c}. Constraint (40c) represents the radar transmit power limitation, with P^{r} denoting the transmit power budget, and constraint (40d) represents the communication transmit power limitation where P^{c} is the transmit power budget. Moreover, (40e) and (40f) represent that the radar can only re-use the spectrum of one small-cell BS.

To address the optimization problem, we propose a PDD-based algorithm for the tracking stage (PA-TS). Similarly, we can simplify problem in (40) by traversing ξ_k, and the problem corresponding to the $\hat{k}$-th BS is formulated as

$$\max_{\{\mathbf{u}_t, \mathbf{s}_{t,l}, \mathbf{w}_{t,\hat{k}}\}} \quad \frac{\sum\limits_{l=1}^{L} \left| \mathbf{u}_{t,l}^{H} \alpha_{\text{t}} e^{j2\pi \frac{q_{\text{t}}}{Q} l} \mathbf{V}_t \mathbf{s}_{t,l} \right|^2}{\sum\limits_{l=1}^{L} \left| \mathbf{u}_{t,l}^{H} \mathbf{G}_{\hat{k}} \mathbf{w}_{t,\hat{k}} \right|^2 + \sigma_{\text{r}}^2 \sum\limits_{l=1}^{L} \left\| \mathbf{u}_{t,l} \right\|^2}, \tag{41a}$$

$$\text{s.t.} \quad \frac{L \left| \mathbf{h}_{\hat{k}}^{H} \mathbf{w}_{t,\hat{k}} \right|^2}{\sum\limits_{l=1}^{L} \left| \mathbf{g}_{\hat{k}}^{H} \mathbf{s}_{t,l} \right|^2 + L \sigma_{\text{c}}^2} \geq \gamma^{\text{c}}, \tag{41b}$$

$$\left\|\mathbf{w}_{t,\hat{k}}\right\|^2 \le P^c, \tag{41c}$$

$$(40c).$$

For the problem in (41) with highly coupled variables, solving the optimal solution for the problem is challenging. Therefore, we adopt a similar approach as the PA-DS algorithm to tackle the problem.

6.2 Proposed algorithm

Firstly, by introducing auxiliary variables and making equivalent substitutions, we transform the problem into a more manageable form. This enables us to simplify the problem and facilitate the subsequent analysis. Since the objective function is fractionally coupled, we introduce an auxiliary variable v_l to reformulate the objective function equivalently as [44],

$$\min_{\left\{\mathbf{s}_{t,l}, \mathbf{w}_{t,\hat{k}}, \mathbf{u}_t, v_l\right\}} \sum_{l=1}^{L} \left(|v_l|^2 \left(\left| \mathbf{u}_{t,l}^H \mathbf{G}_{\hat{k}} \mathbf{w}_{\hat{k}} \right|^2 + \sigma_{\mathrm{r}}^2 \|\mathbf{u}_{t,l}\|^2 \right) - 2\Re(v_l^* \mathbf{u}_{t,l}^H \alpha_{\mathrm{t}} e^{j2\pi \frac{q_{\mathrm{t}}}{Q} l} \mathbf{V}_t \mathbf{s}_{t,l}) \right). \tag{42}$$

Since the optimization variables in (41b) are highly coupled, we use auxiliary variables $\phi, \varphi_l, \forall l$ to perform the following equivalent replacements

$$\phi = \mathbf{h}_{\hat{k}}^H \mathbf{w}_{t,\hat{k}}, \tag{43}$$

$$\varphi_l = \mathbf{g}_{\hat{k}}^H \mathbf{s}_{t,l}. \tag{44}$$

Thus, the constraint (41b) can be rewritten as

$$\gamma^{\mathrm{c}} \left(\sum_{l=1}^{L} |\varphi_l|^2 + L\sigma_{\mathrm{c}}^2 \right) - L|\phi|^2 \le 0. \tag{45}$$

Similar to the detection stage, we introduce AL multipliers $\Gamma_2 = \left\{\lambda_1, \lambda_{2,l}, \forall l\right\}$ to formulate the objective function as

$$\min_{\mathbb{X}_2} \sum_{l=1}^{L} \left(|v_l|^2 \left(\left| \mathbf{u}_{t,l}^H \mathbf{G}_{\hat{k}} \mathbf{w}_{t,\hat{k}} \right|^2 + \sigma_{\mathrm{r}}^2 \|\mathbf{u}_{t,l}\|^2 \right) - 2\Re(v_l^* \mathbf{u}_{t,l}^H \alpha_{\mathrm{t}} e^{j2\pi \frac{q_{\mathrm{t}}}{Q} l} \mathbf{V}_t \mathbf{s}_{t,l}) \right)$$
$$+ \frac{1}{2\rho} \left| \phi - \mathbf{h}_{\hat{k}}^H \mathbf{w}_{t,\hat{k}} + \rho\lambda_1 \right|^2 + \frac{1}{2\rho} \sum_{l=1}^{L} \left| \varphi_l - \mathbf{g}_{\hat{k}}^H \mathbf{s}_{t,l} + \rho\lambda_{2,l} \right|^2, \tag{46a}$$

where $\mathbb{X}_2 = \left\{\mathbf{s}_{t,l}, \mathbf{w}_{t,\hat{k}}, \mathbf{u}_t, \phi, \varphi_l\right\}$ is the set of optimization variables. According to [41], when $\rho \to 0$, the problem in (46) is equivalent to the problem in (41). Then, with the first-order Taylor expansion, $|\phi|^2$ in the j-th iteration can be approximated as

$$|\phi|^2 \approx -\left|\phi^{(j)}\right|^2 + 2\Re\left(\left(\phi^{(j)}\right)^* \phi\right). \tag{47}$$

Thus, the problem in (46) can be reformulated as

$$\min_{\mathbb{X}_2} \sum_{l=1}^{L} \left(|\nu_l|^2 \left(\left| \mathbf{u}_{t,l}^H \mathbf{G}_{\hat{k}} \mathbf{w}_{t,\hat{k}} \right|^2 + \sigma_r^2 \|\mathbf{u}_{t,l}\|^2 \right) - 2\Re(\nu_l^* \mathbf{u}_{t,l}^H \alpha_0 e^{j2\pi \frac{q_t}{Q} l} \mathbf{V}_t \mathbf{s}_{t,l}) \right)$$
$$+ \frac{1}{2\rho} \left| \phi - \mathbf{h}_{\hat{k}}^H \mathbf{w}_{t,\hat{k}} + \rho\lambda_1 \right|^2 + \frac{1}{2\rho} \sum_{l=1}^{L} \left| \varphi_l - \mathbf{g}_{\hat{k}}^H \mathbf{s}_{t,l} + \rho\lambda_{2,l} \right|^2, \tag{48a}$$

$$\text{s.t. } \gamma^c (\sum_{l=1}^{L} |\varphi_l|^2 + L\sigma_c^2) + L\left| \phi^{(j)} \right|^2 - 2L\Re\left(\left(\phi^{(j)} \right)^* \phi \right) \le 0, \tag{48b}$$
$$(40c) \text{ and } (41c),$$

Therefore, to solve the problem in (48), we divide it into several blocks that can be solved with the CCCP-based algorithm and the BCD algorithm. The details of the derivation and complexity analysis are omitted for brevity. In summary, we propose the PA-TS algorithm that solves the problem in (40) using a traversal algorithm. Specifically, we solve the subproblem in (41) using the PDD-based algorithm with a given BS selection and choose the maximum SINR among the SINRs obtained under different BS selections.

7 Numerical simulations

In this section, we conduct comprehensive numerical simulations to thoroughly evaluate and validate the performance of the proposed algorithms.

7.1 Simulation setup

There is a RCC system where eight small-cell BSs are distributed around the radar for communication. Given the current server capabilities and our system's computational requirements, we anticipate a practical computational time of approximately 0.1 s per cycle. The distance between the small-cell BS and the radar is 100 m, and each small-cell BS serves one user within 40 m. Without loss of generality, we consider a co-located MIMO radar with eight transmit antennas and eight receive antennas, i.e., $M_T = M_R = 8$. Each small-cell BS is equipped with eight transmit antennas, i.e., $N_T = 8$. And the space between antennas is $\lambda_0/2$, i.e., $\Delta = \lambda_0/2$. As for the wireless channel with large-scale fading, we have

$$L(d) = 36.7 \log(d) + 32.6, \tag{49}$$

where d is the link distance. We adopt the Rician fading as the small-scale fading [7, 45] which is modeled as

$$\mathbf{H} = \sqrt{\frac{\varepsilon}{1+\varepsilon}} \mathbf{v}_{M_r}(\theta_r) \mathbf{v}_{M_t}(\theta_t)^T + \sqrt{\frac{1}{1+\varepsilon}} \mathbf{H}_0, \tag{50}$$

where ε denotes the Rician factor, M_t, M_r are the numbers of transmit and receive antennas, respectively, θ_T, θ_r represent the corresponding azimuth angles, $\mathbf{H}_0$ is the non-line-of-sight part with each element following the distribution of $\mathcal{CN}(0,1)$. We set $\varepsilon = 3$ dB for both the link from the BS to the radar and the link from the radar to the user, and set $\varepsilon = 9$ dB for the link from the BS to the corresponding user. For MIMO radar, we assume that there are four directions to be detected, i.e., $M = 4$, and the length of transmitted

signal is set as 8, i.e., $L = 8$. At the detection stage, the SINR requirements for radar and communication are both set as 10 dB. At the tracking stage, the communication SINR requirement is 30 dB, the communication transmit power budget is 30 dBm, while the radar transmit power budget is 50 dBm.

We implement several benchmark algorithms for comparison.

- Fixed-Sharing: The radar always re-uses the same spectrum, and the best of K options are chosen.
- Randomized-Sharing: In this case, the radar system randomly selects a small-cell BS to re-use its spectrum.
- MMSE-Centric: The system is jointly designed except that the beamforming vector $\mathbf{w}_{\hat{k}}$ of the communication system is given by the minimum mean square error (MMSE) algorithm [46].

7.2 Convergence performance

Now we investigate the convergence of the proposed PDD-based algorithm to problem in (23).

The convergence performance of the proposed PDD-based algorithm is shown in Fig. 5. First, the transmit power converges to around 300 W after 10 iterations, indicating that the algorithm has reached a stationary point of the original problem. Additionally, in the 9-th iteration, the violation indicator which is defined in (36) and used in the inner loop rapidly converges to around 0.5, thus confirming the fast convergence of the proposed algorithm, and the computed results are reliable in the subsequent iterations.

7.3 Radar target detection

In the subsequent section, we conduct a performance evaluation of various algorithms at the detection stage. Figure 6 illustrates the probability of obtaining a feasible solution versus γ^{r}. In Figure 6, the y-axis represents the probability that the system achieves a feasible solution meeting all optimization constraints. This indicates how likely our joint design approach is to successfully meet the system requirements under various conditions. The results indicate that the PA-DS algorithm achieves the highest probability of obtaining a feasible solution, which is almost equal to 1. In contrast, the Randomized-Sharing algorithm exhibits the lowest probability of obtaining a feasible solution. Since the MMSE-Centric algorithm prioritizes communication requirements, which may lead to less flexibility in accommodating the radar's SINR requirements. As the SINR requirement increases, the MMSE-Centric approach must work harder to balance communication needs, which might be increasingly at odds with the radar's requirements. This can lead to a decrease in the probability of finding a feasible solution as it becomes more challenging to satisfy the higher radar SINR requirements while still maintaining communication quality. By contrast, the proposed algorithm outperforms the benchmark algorithms and exhibits superior performance in acquiring feasible solutions.

Figure 7 illustrates the impact of the radar SINR requirement, i.e., γ^{r}, on the system transmit power. Firstly, all four algorithms exhibit an increase in system power as γ^{r} increases. Secondly, the system power of the PA-DS algorithm is always the lowest,

Mao *et al. J Wireless Com Network* (2024) 2024:56
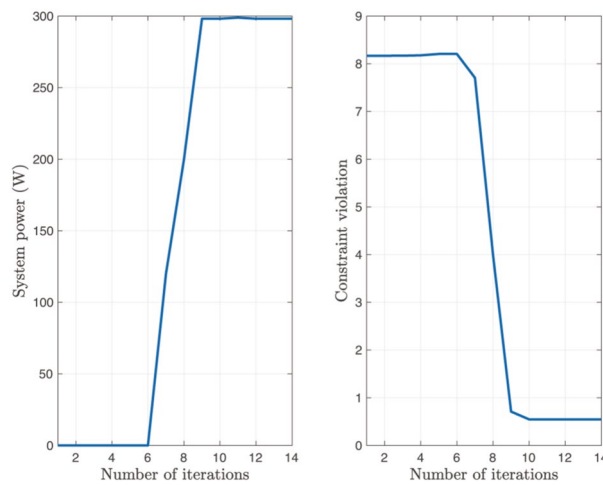
Page 22 of 28

Fig. 5 Convergence performance of the proposed PDD-based algorithm
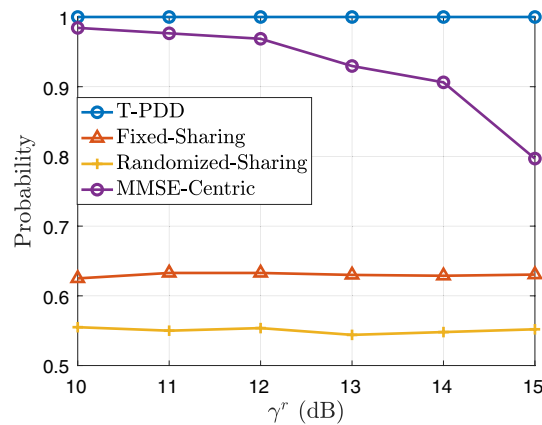

Fig. 6 Probability of obtaining a feasible solution versus γ^r

which demonstrates its best performance compared with others, and the performance gain increases as the γ^r increases. Thirdly, the system power of the MMSE-Centric algorithm is the largest when γ^r is small, while the system power of the Randomized-Sharing algorithm is the largest when γ^r is large. The MMSE-Centric algorithm is primarily designed to optimize the communication quality, and it neglects the interference that the communication system may impose on the radar. As a result, the radar has to increase its transmit power to meet its requirements under low radar SINR conditions. However, as the radar SINR requirement rises, the interference originating from the radar to the communication system becomes more prominent. In this scenario, the MMSE-Centric algorithm that prioritizes communication quality performs better than the Randomized-Sharing algorithm.

The impact of the communication SINR requirement, i.e., γ^c, on the system power is shown in Fig. 8. First, the system power of all four algorithms increases with γ^c as the communication system needs more transmit power to ensure the communication quality. Meanwhile, as the interference from the communication system to the radar
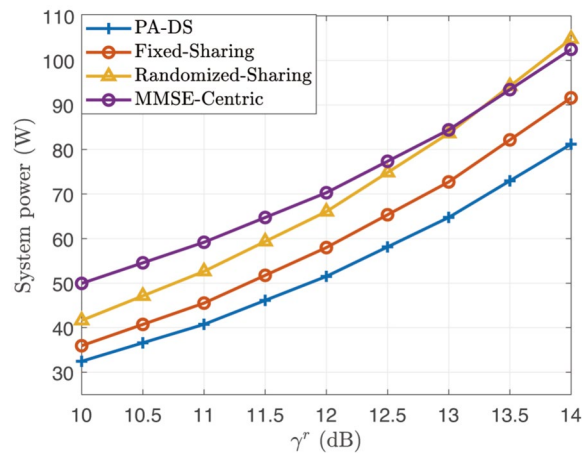
Fig. 7 Total system transmit power versus γ^r

increases, the radar has to increase its transmit power to ensure reliable sensing performance. Secondly, the system power of the MMSE-Centric algorithm improves slowly since it mainly focuses on the satisfaction of communication quality and presents the best performance under low communication SINR requirement. Finally, we can see that the system power of the proposed PA-DS algorithm is always the lowest, demonstrating its superior performance compared to other algorithms.

7.4 Radar target tracking

We compare the performance at the tracking stage for different algorithms.

Figure 9 depicts the performance of radar SINR versus the radar transmit power budget, i.e., P^r. Notably, the PA-TS algorithm demonstrates superior performance, followed by the MMSE-Centric algorithm, whereas the Randomized-Sharing algorithm exhibits the least favorable performance.

The impact of the communication transmit power budget on the radar SINR is depicted in Fig. 10. First of all, it can be observed that the PA-TS algorithm always keeps the best performance, followed by the MMSE-Centric algorithm and the Fixed-Sharing algorithm. Secondly, under a low communication power budget, the MMSE-Centric system achieves a high radar SINR, and the gap between it and the PA-TS algorithm is very small. The reason is that the MMSE-Centric algorithm focuses on ensuring communication quality. In this case, the transmit power can be controlled and thus the interference to the radar is indirectly controlled.

7.5 Parameter estimation

Now, we demonstrate the performance of the proposed SIC-based parameter estimation algorithm as compared against the algorithm without SIC. Figure 11 shows the root-mean-square error (RMSE) of distance and velocity estimation versus radar SINR requirement, i.e., γ^r. From Fig. 11a, the SIC-based parameter estimation algorithm can always reduce the estimation error of distance to about 10 percent of the algorithm without SIC for different SINR requirements. The RMSE of 20 ms observed, falls within a single-range resolution unit, which validates the effectiveness of our approach. Similarly, as
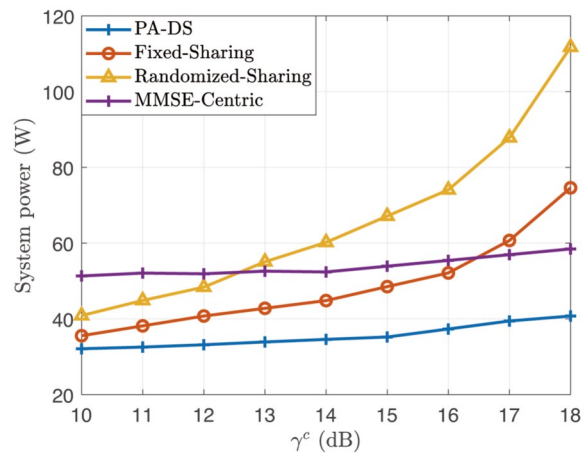
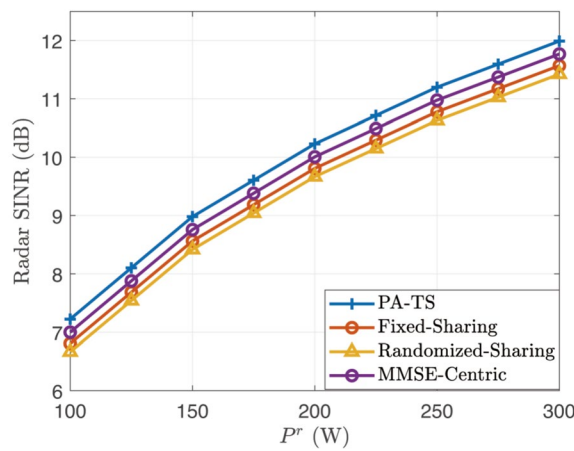**Fig. 8** Total system transmit power versus γ^c

Fig. 9 Radar SINR versus P^r

shown in Fig. 11b, the SIC-based parameter estimation algorithm exhibits significantly reduced target velocity estimation error, validating its superior performance. Accordingly, the proposed algorithm outperforms the algorithm without SIC, thereby substantially enhancing the estimation performance.

8 Conclusion

In this paper, we have considered a RCC system where the radar covers multiple small-cell BSs and chooses one small-cell BS to re-use its spectrum. We have proposed a RCC system framework composed of two stages to realize radar target detection and radar target tracking. At the detection stage, a system transmit power minimization problem has been formulated subject to radar SINR requirement and communication SINR requirement. At the tracking stage, a optimization problem aimed at maximizing the radar SINR subject to communication SINR requirement and transmit power budget has been formulated. To solve the non-convex problems, we equivalently transformed the problem into a more tractable form and proposed a
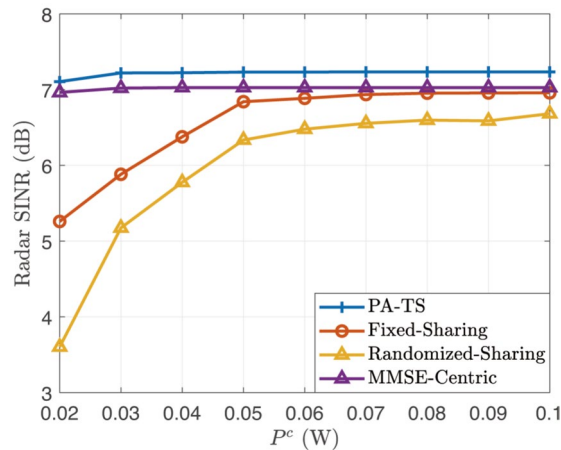
Mao *et al. J Wireless Com Network* (2024) 2024:56

Page 25 of 28

Fig. 10 Radar SINR versus P^c
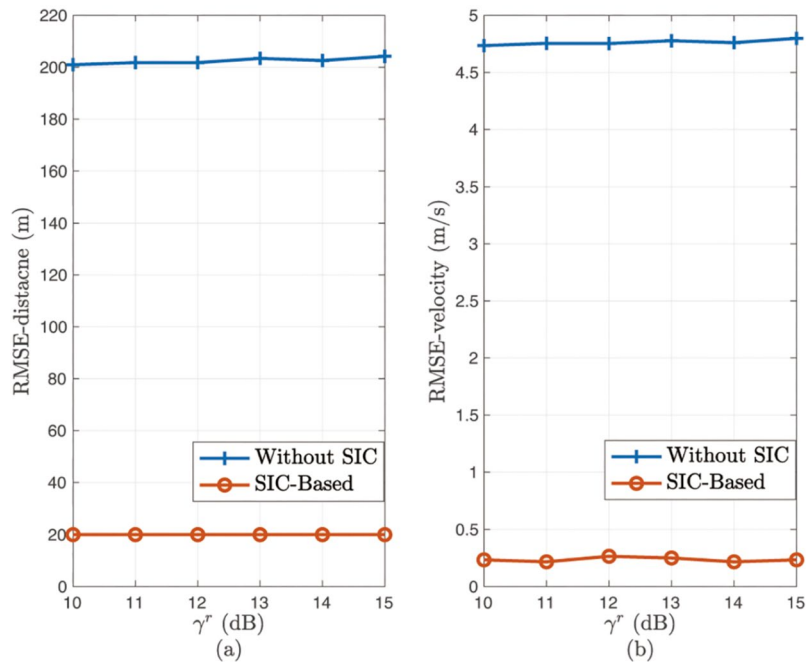

Fig. 11 RMSE of estimation error versus γ^r

PDD-based algorithm with double-layer loop. In the inner loop, we utilize the CCCP algorithm for solving the AL problem and the BCD algorithm for updating the system variables. In the outer loop, the penalty factors or AL multipliers are updated. Furthermore, to address the interference of the communication system on radar, we proposed a SIC-based algorithm for radar target parameter estimation and update. Finally, numerical experiments were conducted to validate the performance of the proposed algorithms, demonstrating that the PDD-based algorithm ensures feasible solutions and outperforms several benchmark algorithms. Additionally, the superiority of the SIC-based parameter estimation algorithm was confirmed.

9 Results and discussion

This paper proposes a noval RCC system framework composed of detection stage and tracking stage. And a PDD-based algorithm is proposed to solve the AL problem in the inner loop. Furthermore, we propose a SIC-based algorithm to improve the performance of parameter estimation. However, this paper only considers that each BS serves for one user which is equipped with single antenna. However, real-world communication networks are often more intricate, involving multiple users interacting with each BS. This complexity arises from the need to efficiently manage the increasing volume of data traffic and the diverse communication requirements of modern users. Future research will extend to exploring more complex communication systems.

Abbreviations

BS	Base station
PDD	Penalty dual decomposition
CCCP	Concave–convex procedure
BCD	Block coordinate descent
SIC	Successive interference cancellation
RCC	Radar-communication coexistence
DFRC	Dual-functional radar communication
MIMO	Multiple-input multiple-output
TDD	Time division duplex
OTFS	Orthogonal time frequency space
MISO	Multiple-input single-output
PRI	Pulse repetition interval
SINR	Signal-to-interference-plus-noise ratio
JD-DS	Joint design of the detection stage
PE	Parameter estimation
PP	Parameter prediction
JS-TS	Joint design of the tracking stage
MUSIC	Multiple signal classification
MF	Matched filter
PA-DS	PDD-based algorithm for the detection stage
LFM	Linear frequency modulation
PA-TS	PDD-based algorithm for the tracking stage
MMSE	Minimum mean square error
RMSE	Root-mean-square error

Declarations

Competing interests
The authors declare that they have no conflict of interest.

References
1.   M.A. Govoni, Enhancing spectrum coexistence using radar waveform diversity, in *Proc. IEEE Radar Conference (RadarConf 2016)*, pp. 1–5 (2016)

2. H. Griffiths, S. Blunt, L. Cohen, L. Savy, Challenge problems in spectrum engineering and waveform diversity, in *Proceedings of the IEEE Radar Conference (RadarCon 2013)*, pp. 1–5 (2013)
3. B. Paul, A.R. Chiriyath, D.W. Bliss, Survey of RF communications and sensing convergence research. IEEE Access **5**, 252–270 (2017)
4. L. Zheng, M. Lops, Y.C. Eldar, X. Wang, Radar and communication coexistence: an overview: a review of recent methods. IEEE Signal Process Mag. **36**(5), 85–99 (2019)
5. A.R. Chiriyath, B. Paul, D.W. Bliss, Radar-communications convergence: coexistence, cooperation, and co-design. Trans. Cogn. Commun. Netw. **3**(1), 1–12 (2017)
6. J. Qian, M. Lops, L. Zheng, X. Wang, Z. He, Joint system design for coexistence of MIMO radar and MIMO communication. IEEE Trans. Signal Process. **66**(13), 3504–3519 (2018)
7. Y. He, Y. Cai, H. Mao, G. Yu, RIS-assisted communication radar coexistence: joint beamforming design and analysis. IEEE J. Sel. Areas Commun. **40**(7), 2131–2145 (2022)
8. A. Hassanien, M.G. Amin, Y.D. Zhang, F. Ahmad, Signaling strategies for dual-function radar communications: an overview. IEEE Aerosp. Electron. Syst. Mag. **31**(10), 36–45 (2016)
9. F. Liu, L. Zhou, C. Masouros, A. Li, W. Luo, A. Petropulu, Toward dual-functional radar-communication systems: optimal waveform design. IEEE Trans. Signal Process. **66**(16), 4264–4279 (2018)
10. F. Liu, C. Masouros, H. Griffiths, Dual-functional radar-communication waveform design under constant-modulus and orthogonality constraints, in *Proceedings of the Sensor Signal Processing Defence Conference (SSPD 2019)*, pp. 1–5 (2019)
11. R. Liu, M. Li, Q. Liu, A.L. Swindlehurst, Dual-functional radar-communication waveform design: a symbol-level precoding approach. IEEE J. Sel. Top. Signal Process. **15**(6), 1316–1331 (2021)
12. F. Liu, C. Masouros, A tutorial on joint radar and communication transmission for vehicular networks-part I: background and fundamentals. IEEE Commun. Lett. **25**(2), 322–326 (2021)
13. M. Temiz, E. Alsusa, M.W. Baidas, A dual-functional massive MIMO OFDM communication and radar transmitter architecture. IEEE Trans. Veh. Technol. **69**(12), 14974–14988 (2020)
14. F. Liu, C. Masouros, A. Li, T. Ratnarajah, J. Zhou, MIMO radar and cellular coexistence: a power-efficient approach enabled by interference exploitation. IEEE Trans. Signal Process. **66**(14), 3681–3695 (2018)
15. F. Liu, C. Masouros, A. Li, T. Ratnarajah, Robust MIMO beamforming for cellular and radar coexistence. IEEE Wirel. Commun. Lett. **6**(3), 374–377 (2017)
16. B. Li, A.P. Petropulu, W. Trappe, Optimum co-design for spectrum sharing between matrix completion based MIMO radars and a MIMO communication system. IEEE Trans. Signal Process. **64**(17), 4562–4575 (2016)
17. A.F. Martone, K.A. Gallagher, K.D. Sherbondy, Joint radar and communication system optimization for spectrum sharing, in *Proceedings of the IEEE Radar Conference (RadarConf 2019)*, pp. 1–6 (2019)
18. S. Amuru, R.M. Buehrer, R. Tandon, S. Sodagari, MIMO radar waveform design to support spectrum sharing, in *Proceedings of the Military Communications Conference (MILCOM 2013)*, pp. 1535–1540 (2013)
19. A. Khawar, A. Abdel-Hadi, T.C. Clancy, Spectrum sharing between S-band radar and LTE cellular system: a spatial approach, in *Proceedings of the IEEE International Symposium on Dynamic Spectrum Access Networks (DYSPAN 2014)*, pp. 7–14 (2014)
20. C. Shahriar, A. Abdelhadi, T. C. Clancy, Overlapped-MIMO radar waveform design for coexistence with communication systems, in *Proceedings of the IEEE Communications and Networking Conference (WCNC 2015)*, pp. 223–228 (2015)
21. H. Deng, B. Himed, Interference mitigation processing for spectrum-sharing between radar and wireless communications systems. IEEE Trans. Aerosp. Electron. Syst. **49**(3), 1911–1919 (2013)
22. B. Li, H. Kumar, A.P. Petropulu, A joint design approach for spectrum sharing between radar and communication systems, in *Proceedings of the IEEE International Conference on Acoustics, Speech, and Signal Processing (ICASSP 2016)*, pp. 3306–3310 (2016)
23. B. Li, A.P. Petropulu, Joint transmit designs for coexistence of MIMO wireless communications and sparse sensing radars in clutter. IEEE Trans. Aerosp. Electron. Syst. **53**(6), 2846–2864 (2017)
24. L. Zheng, M. Lops, X. Wang, E. Grossi, Joint design of overlaid communication systems and pulsed radars. IEEE Trans. Signal Process. **66**(1), 139–154 (2018)
25. F. Wang, H. Li, M.A. Govoni, Power allocation and co-design of multicarrier communication and radar systems for spectral coexistence. IEEE Trans. Signal Process. **67**(14), 3818–3831 (2019)
26. F. Dong, F. Liu, Y. Cui, W. Wang, K. Han, Z. Wang, Sensing as a service in 6G perceptive networks: a unified framework for ISAC resource allocation. IEEE Trans. Commun. **22**(5), 3522–3536 (2023)
27. F. Liu, C. Masouros, A.P. Petropulu, H. Griffiths, L. Hanzo, Joint radar and communication design: applications, state-of-the-art, and the road ahead. IEEE Trans. Commun. **68**(6), 3834–3862 (2020)
28. F. Liu, W. Yuan, C. Masouros, J. Yuan, Radar-assisted predictive beamforming for vehicular links: communication served by sensing. IEEE Trans. Wirel. Commun. **19**(11), 7704–7719 (2020)
29. F. Liu, C. Masouros, A tutorial on joint radar and communication transmission for vehicular networks-part II: state of the art and challenges ahead. IEEE Commun. Lett. **25**(2), 327–331 (2021)
30. Marian Bică, Visa Koivunen, Radar waveform optimization for target parameter estimation in cooperative radar-communications systems. IEEE Trans. Aerosp. Electron. Syst. **55**(5), 2314–2326 (2018)
31. L. Gaudio et al., On the effectiveness of OTFS for joint radar parameter estimation and communication. IEEE Trans. Wirel. Commun. **19**(9), 5951–5965 (2020)
32. D. Halperin, T. Anderson, D. Wetherall, Taking the sting out of carrier sense: interference cancellation for wireless lans, in *Proceedings 14th ACM MobiCom*, pp. 339–350 (2018)
33. N.-T. Le, L.-N. Tran, Q.-D. Vu, D. Jayalath, Energy-efficient resource allocation for OFDMA heterogeneous networks. IEEE Trans. Commun. **67**(10), 7043–7057 (2019)
34. F. Wang, W. Chen, H. Tang, Q. Wu, Joint optimization of user association, subchannel allocation, and power allocation in multicell multi-association OFDMA heterogeneous networks. IEEE Trans. Commun. **65**(6), 2672–2684 (2017)
35. S. Coleri, M. Ergen, A. Puri, A. Bahai, Channel estimation techniques based on pilot arrangement in OFDM systems. IEEE Trans. Broadcas. **48**(3), 223–229 (2002)

36. S.G. Kang, Y.M. Ha, E.K. Joo, A comparative investigation on channel estimation algorithms for OFDM in mobile communications. IEEE Trans. Broadcast. **49**(2), 142–149 (2003)
37. P. Gupta, S.P. Kar, MUSIC and improved MUSIC algorithm to estimate direction of arrival, in *Proceedings of the International Conference on Communication and Signal Process (ICCSP 2015)*, pp. 757–761 (2015)
38. O. Aldayel, V. Monga, M. Rangaswamy, Successive QCQP refinement for MIMO radar waveform design under practical constraints. IEEE Trans. Signal Process. **64**(14), 3760–3774 (2016)
39. G.R. Curry, *Radar System Performance Modeling* (Artech House, Norwood, 2005)
40. D. Bertsekas, *Nonlinear Programming*, 2nd edn. (Athena Scientific, Belmont, 1999)
41. Q. Shi, M. Hong, Penalty dual decomposition method for non-smooth nonconvex optimization-part I: algorithms and convergence analysis. IEEE Trans. Signal Process. **68**, 4108–4122 (2020)
42. Q. Shi, M. Hong, Penalty dual decomposition method with application in signal processing, in *Proceedings of the International Conference on Acoustics, Speech and Signal Process (ICASSP 2017)*, pp. 4059–4063 (2017)
43. A.L. Yuille, A. Rangarajan, The concave–convex procedure. Neural Comput. **15**(4), 915–936 (2003)
44. K. Shen, W. Yu, Fractional programming for communication systems-part I: power control and beamforming. IEEE Trans. Signal Process. **66**(10), 2616–2630 (2018)
45. S. Pratschner, T. Blazek, E. Zchmann et al., A spatially consistent MIMO channel model with adjustable k factor. IEEE Access **7**, 110174–110186 (2019)
46. Y.C. Eldar, A. Nehorai, P.S. La Rosa, A competitive mean-squared error approach to beamforming. IEEE Trans. Signal Process. **55**(11), 5143–5154 (2007)

Publisher's Note

Springer Nature remains neutral with regard to jurisdictional claims in published maps and institutional affiliations.